

ornl

**OAK RIDGE
NATIONAL
LABORATORY**

MARTIN MARIETTA

OPERATED BY
MARTIN MARIETTA ENERGY SYSTEMS, INC.
FOR THE UNITED STATES
DEPARTMENT OF ENERGY

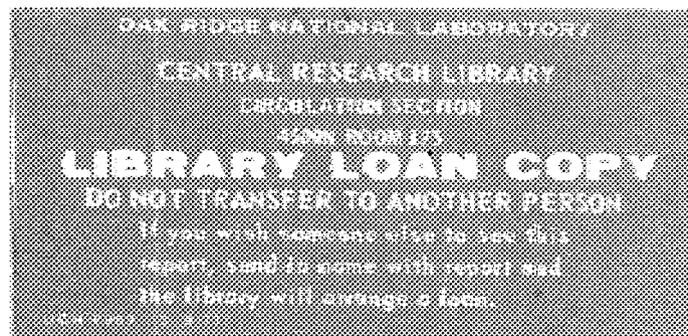


3 4456 0069237 4

ORNL/TM-10093

Recent Improvements of the TNG Statistical Model Code

K. Shibata
C. Y. Fu



Printed in the United States of America. Available from
National Technical Information Service
U. S. Department of Commerce
5285 Port Royal Road, Springfield, Virginia 22161
NTIS price codes—Printed Copy: A03; Microfiche A01

This report was prepared as an account of work sponsored by an agency of the United States Government. Neither the United States Government nor any agency thereof, nor any of their employees, makes any warranty, express or implied, or assumes any legal liability or responsibility for the accuracy, completeness, or usefulness of any information, apparatus, product, or process disclosed, or represents that its use would not infringe privately owned rights. Reference herein to any specific commercial product, process, or service by trade name, trademark, manufacturer, or otherwise, does not necessarily constitute or imply its endorsement, recommendation, or favoring by the United States Government or any agency thereof. The views and opinions of authors expressed herein do not necessarily state or reflect those of the United States Government or any agency thereof.

Engineering Physics and Mathematics Division

RECENT IMPROVEMENTS OF THE TNG STATISTICAL MODEL CODE

K. Shibata* and C. Y. Fu

Manuscript Completed: June 1, 1986
Date Published: August 1986

*Japan Atomic Energy Research Institute, Japan

NOTICE This document contains information of a preliminary nature.
It is subject to revision or correction and therefore does not represent a
final report.

Prepared by the
OAK RIDGE NATIONAL LABORATORY
Oak Ridge, Tennessee 37831
operated by
Martin Marietta Energy Systems, Inc.
Under Contract No. DE-AC05-84OR21400
for the
Division of Basic Energy Sciences



3 4456 0069237 4

CONTENTS

Abstract	1
1. Introduction	2
2. Variable Bin Widths for Outgoing-Particle Energies	2
3. Capture Gamma-Ray Spectra	5
4. Precompound Mode of (n,γ) Reaction	5
5. Fission	7
6. Summary	9
Acknowledgements	12
References	12
Appendix A. Explanation of Input Data for TNG	13
Appendix B. Input Data for Sample Calculations	27

RECENT IMPROVEMENTS OF THE TNG STATISTICAL MODEL CODE*

K. Shibata
Japan Atomic Energy Research Institute, Japan

C. Y. Fu
Engineering Physics and Mathematics Division

ABSTRACT

The applicability of the nuclear model code TNG to cross-section evaluations has been extended. The new TNG is capable of using variable bins for outgoing particle energies. Moreover, three additional quantities can now be calculated: capture gamma-ray spectrum, the precompound mode of the (n,γ) reaction, and fission cross section. In this report, the new features of the code are described together with some sample calculations and a brief explanation of the input data.

* This work was performed under the cooperative program between the United States Department of Energy and the Japan Atomic Energy Research Institute in the area of nuclear physics.

I. INTRODUCTION

Theoretical calculation plays an important role in evaluating nuclear data. The statistical-model calculation is frequently performed for medium and heavy nuclei. The TNG code¹ is a multistep statistical model code based on the Hauser-Feshbach theory² including width-fluctuation corrections and precompound effects. This code has been used³ for the evaluation of neutron data at the Oak Ridge National Laboratory since 1972. In the course of these evaluations, the code has been continuously improved (see ref. 4) in order to determine the neutron cross sections more accurately. In this report we describe the most recent improvements.

The original TNG used constant (equi-distant) bins for outgoing particle energies. In order to use the code on small computers, such as a PDP-10, the number of bins per reaction was restricted to 40. The resulting bins can be too wide, particularly near the $(n,2n)$ threshold and can lead to energy-balance problems.⁵ To alleviate these problems, we developed a scheme that allowed the bin widths to vary with the outgoing particle energies. For the (n,γ) reaction, two additional quantities can now be calculated: the gamma-ray production spectrum and the precompound cross section. The precompound mode of (n,γ) reaction was indispensable not only to reproduce the experimental data in the MeV region but also to keep consistency with particle emission in the precompound mode. In the case of fissionable nuclei, theoretical estimates of the fission cross sections are essential for evaluating the neutron cross sections, but the original code did not have this capability. The present work is an attempt to satisfy all these requirements.

In this report each of the new features of TNG is described together with some sample calculations. A brief explanation of input data for the new TNG code is given in Appendix A. The input data for the sample cases are presented in Appendix B. These appendices are intended for internal use only. A user's guide for TNG is in preparation.

2. VARIABLE BIN WIDTHS FOR OUTGOING-PARTICLE ENERGIES

The original TNG employed a constant binning method for outgoing-particle energies. A bin width of 0.5 MeV was usually used for incident energies between 15 and 20 MeV in the calculation. The width was, however, too large to calculate the neutron emission spectra accurately at low outgoing energies, particularly near the $(n,2n)$ and $(n,3n)$ reaction thresholds. This is why some energy balance problems had occurred in the copper evaluation.⁵ Obviously such problems will be solved if we can use bins small enough to maintain the accuracy of calculated cross sections at low energies. If we do so, the evaluation will become more costly because much more computer time and memory are needed. From a practical viewpoint, that is not preferable. Therefore, we decided to adopt variable bins, i.e., smaller bins at low outgoing-particle energies and larger ones at high outgoing-particle energies, instead of constant bins.

As an example, the neutron cross sections of ⁵⁶Fe were calculated at 14.5 MeV with the input data used in a recent analysis⁴ for ⁵⁶Fe. The calculated cross sections are presented in Table 1, where comparison of the binning methods is performed. It is obvious from the table that the calculated cross sections hardly depend on the binning methods, and this indicates that a change in the spectral shape has little effect on the integrated cross sections. The neutron and proton spectra are shown in Figs. 1 and 2, respectively. In Fig. 1, the spectrum below 500 keV is much better defined with the variable binning than with the constant bins of 0.5 MeV, and there is no marked difference above 5 MeV where the widths of the variable bins become wider. Use of the variable binning also induces a change in the proton spectrum near the threshold energy, as seen in Fig. 2.

Table 1. Comparison of 14.5 MeV cross sections of ^{56}Fe calculated with variable and constant bins. The cross sections are in mb.

Reaction	Variable-bin case	Constant-bin case
1st Step		
(n, n') Disc. ^a	122.6	122.9
(n, n') Cont. ^b	1066.4	1066.7
(n, n') Total	1189.0	1189.6
(n, p) Disc.	3.2	2.0
(n, p) Cont.	128.2	129.3
(n, p) Total	131.4	131.3
(n, α) Disc.	2.8	2.8
(n, α) Cont.	42.4	41.9
(n, α) Total	45.2	44.7
2nd Step		
$(n, n\gamma)$	692.0	691.0
$(n, 2n)$	456.9	460.8
(n, np)	39.6	37.5
$(n, n\alpha)$	0.5	0.5
$(n, p\gamma)$	105.5	105.8
(n, pn)	25.9	25.4
$(n, \alpha\gamma)$	43.8	43.4
$(n, \alpha n)$	1.4	1.3

^aSum of discrete energy transitions.

^bSum of continuum transitions.

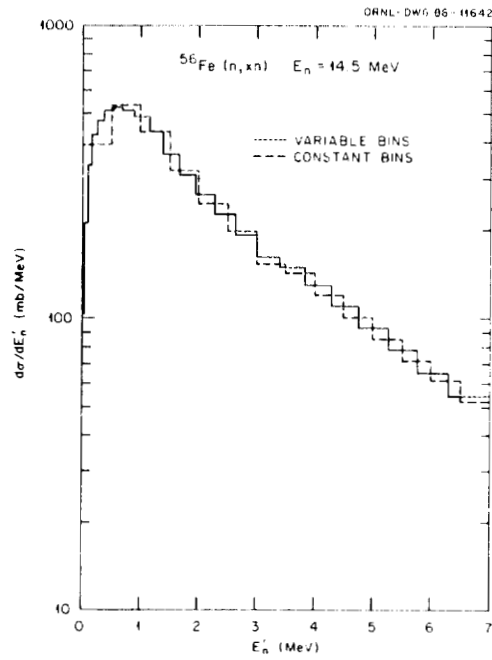


Fig. 1. Neutron spectra emitted from the $n + ^{56}\text{Fe}$ reaction at 14.5 MeV. The solid line stands for the calculation with variable binning, while the dashed line is that with constant binning.

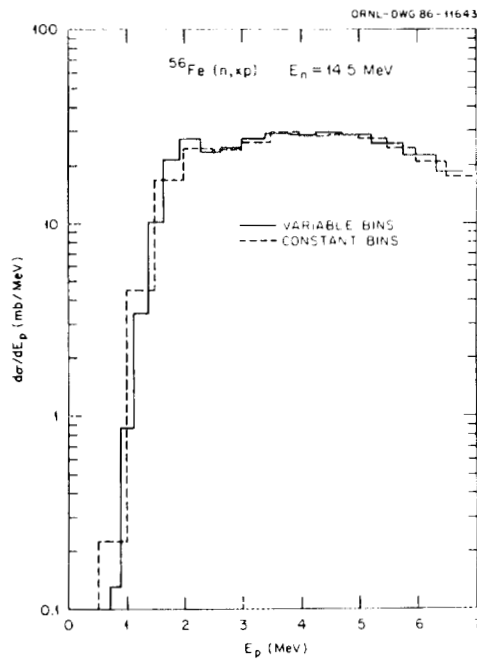


Fig. 2. Proton spectra emitted from the $n + ^{56}\text{Fe}$ reaction at 14.5 MeV. The two lines have the same meaning as in Fig. 1.

3. CAPTURE GAMMA-RAY SPECTRA

Capture gamma-ray spectra are particularly important for shielding calculations. The original TNG could not predict them, although it could give the cascade gamma-ray spectra accompanied by particle emission. The present work has made it possible to calculate the capture spectra using TNG. A special care was taken to estimate the branching ratios for primary transitions from the capture state to the discrete levels of the compound nucleus. Generally speaking, some s-wave branching ratios have been determined by measurements but are incomplete, and hence a partial theoretical prediction is required. With the new code, if the sum of the gamma-ray transition probabilities determined experimentally is less than unity, the giant-dipole model calculation is applied to obtain the missing gamma-ray transitions. Gamma-ray spectra due to p-wave capture, d-wave capture, etc., are entirely from theoretical predictions.

As an example, the gamma-ray spectra from the $^{56}\text{Fe}(n,\gamma)$ reaction was calculated at 100 keV, and the results are shown in Fig. 3. The solid line takes into account the experimental s-wave branching ratios compiled by Auble⁶ for primary transitions. The sum of them was found to be 0.71, and 29% of the primary transitions was therefore determined theoretically. The dotted line is the case that considers the theoretical prediction alone. Marked differences between the two curves are seen in the regions above 5 MeV and below 2 MeV. The high-energy portion corresponds to the transitions from the captured state to the discrete levels of ^{57}Fe , while the low-energy portion is attributed to the transitions among the discrete levels. At 100 keV, the s-wave capture cross section amounts to 86% of the total capture cross section, hence the input s-wave branching ratios played a large role. As the incident neutron energy increases, the s-wave strength will decrease and the calculated capture spectrum will depend more and more on theoretical prediction.

4. PRECOMPOUND MODE OF (n,γ) REACTION

The precompound component of the capture cross section is represented by

$$d\sigma_{n,\gamma}/d\epsilon = \sigma_{cN} \sum_{ph} W_{\gamma}(p,h,\epsilon) \int_0^T P(p,h,t) dt \quad , \quad (1)$$

where σ_{cN} is the compound-nucleus formation cross section and $W_{\gamma}(p,h,\epsilon)$ is the gamma-ray emission rate with an energy ϵ from a nucleus in the p -particle and h -hole state. The quantity $P(p,h,t)$ is the occupation probability of a state with p -particles and h -holes at time t , and T is the equilibration time when all states in the composite system are equally populated. The gamma-ray emission rate $W_{\gamma}(p,h,\epsilon)$ was derived by Akkermans and Gruppelaar:⁷

$$W_{\gamma}(p,h,\epsilon) = \frac{\epsilon^2}{\pi^2 \hbar^3 c^2} \sigma_{inv}(\epsilon) \frac{1}{\omega(p,h,E)} \left[\frac{\omega(1,1,\epsilon)\omega(p-1,h-1,E-\epsilon)}{g(p+h-2) + \omega(1,1,\epsilon)} + \frac{g(p+h)\omega(p,h,E-\epsilon)}{g(p+h) + \omega(1,1,\epsilon)} \right] \quad (2)$$

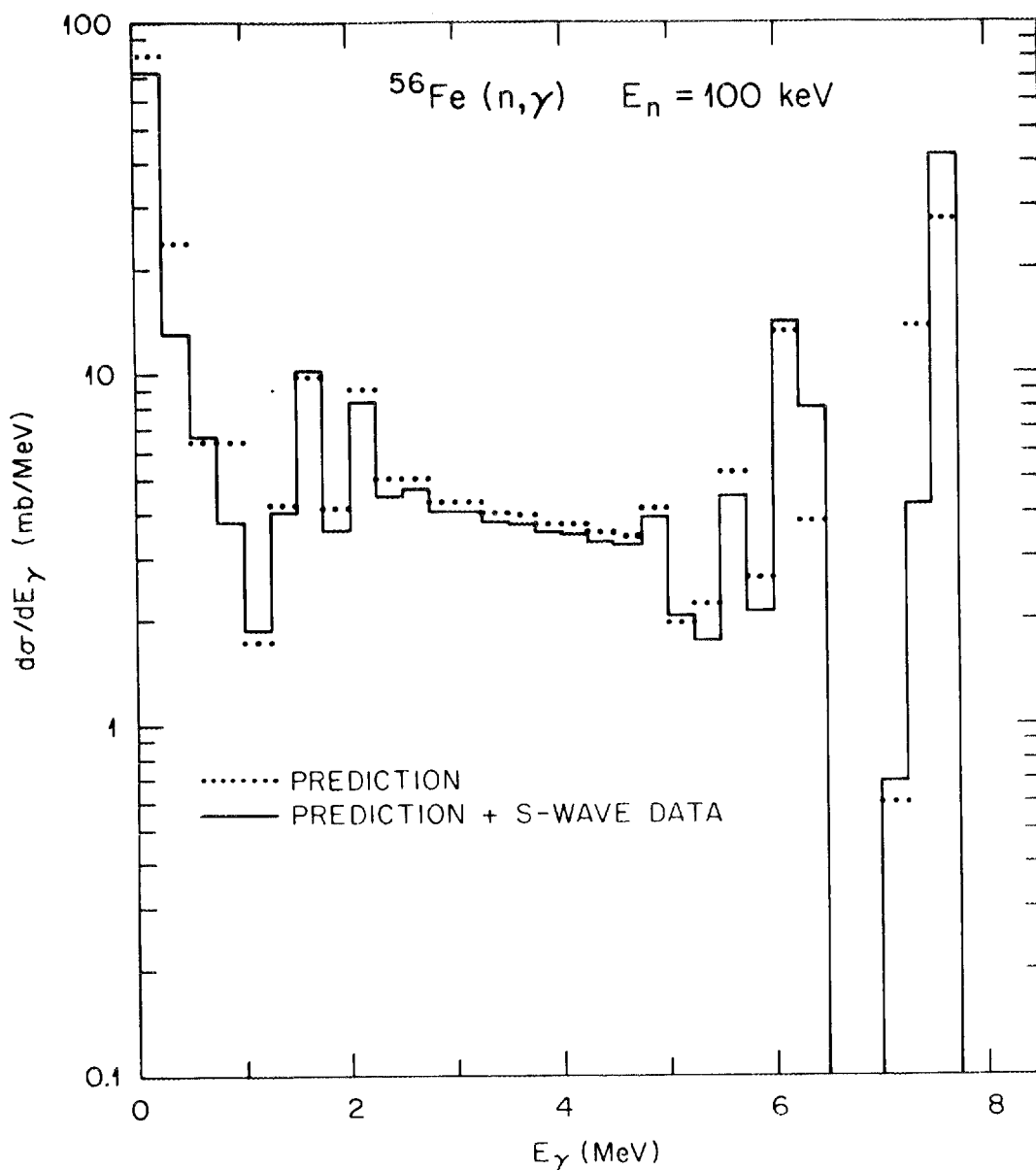


Fig. 3. Gamma-ray spectra emitted from the $^{56}\text{Fe}(n, \gamma)$ reaction at 100 keV. The dotted histogram is 100% prediction. The solid histogram is partial prediction in which 71% of the calculated *s*-wave transitions has been replaced by input transitions compiled (ref. 6) from thermal neutron capture data.

The symbols used in Eq. (2) are defined as follows:

E	=	the excitation energy in the compound nucleus,
\hbar	=	Planck constant,
c	=	light velocity,
$\sigma_{inv}(\epsilon)$	=	the inverse reaction cross sections at an energy ϵ ,
g	=	the single-particle state density, and
$\omega(p, h, \epsilon)$	=	the state density with p -particles and h -holes at ϵ .

The state density $\omega(p, h, E)$ is given by

$$\omega(p, h, E) = \frac{g(gE - A_{p,h})^{p+h-1}}{p! h! (p+h-1)!} \quad (3)$$

where $A_{p,h} = (p_2 + h^2 - p - h)/4$. The inverse reaction cross section σ_{inv} is calculated with the giant-dipole model. The master equations solved previously¹ in TNG were modified to start with the $1p-0h$ state, because the direct capture corresponds to the $1p-0h$ configuration.

As a test case, the capture cross section of ⁹³Nb was calculated. Figure 4 shows the calculated results together with an experimental data point. There is one scaling factor for the precompound (n, γ) reaction, and a good fit to the measurement was obtained by adjusting this factor. In this case, the factor was found to be 1.0. The capture gamma-ray spectra are shown in Fig. 5, where the direct capture calculation by Rigaud et al.⁸ is also illustrated. The present calculation reproduces the experimental data satisfactorily. The precompound capture method is simple to use and appears capable of adequately representing the direct capture mechanism in cross-section evaluation work.

5. FISSION

Two models were applied to calculate the fission cross sections: the single-humped barrier⁹ and the double-humped barrier¹⁰ models.

In the single-humped barrier model, the transmission coefficient is given by¹¹

$$T_f^{J\pi} = \sum_{\mu} \left[1 + \exp\{-(2\pi/\hbar\omega)(E - E_f - E_{\mu}^{J\pi})\} \right]^{-1} + \int_0^{\infty} d\epsilon \rho(\epsilon, J\pi) \frac{1}{1 + \exp\{-(2\pi/\hbar\omega)(E - E_f - \epsilon)\}} \quad (4)$$

where E is the excitation energy, E_f the fission barrier energy, and $E_{\mu}^{J\pi}$ the discrete level energy with spin and parity of $J\pi$. The quantity $\rho(\epsilon, J\pi)$ is the level density at ϵ , and $\hbar\omega$ represents the curvature of the barrier.

On the other hand, in the double-humped barrier model, the transmission coefficient is given by

$$T_f^{J\pi} = T_A^{J\pi} T_B^{J\pi} / (T_A^{J\pi} + T_B^{J\pi}) \quad (5)$$

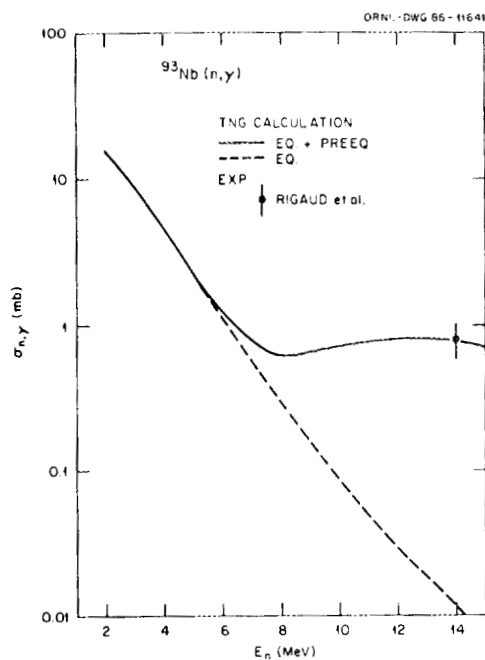


Fig. 4. Capture cross section of ^{93}Nb in the MeV region. The solid line is the sum of the compound and precompound contributions. The dashed line is the compound contribution.

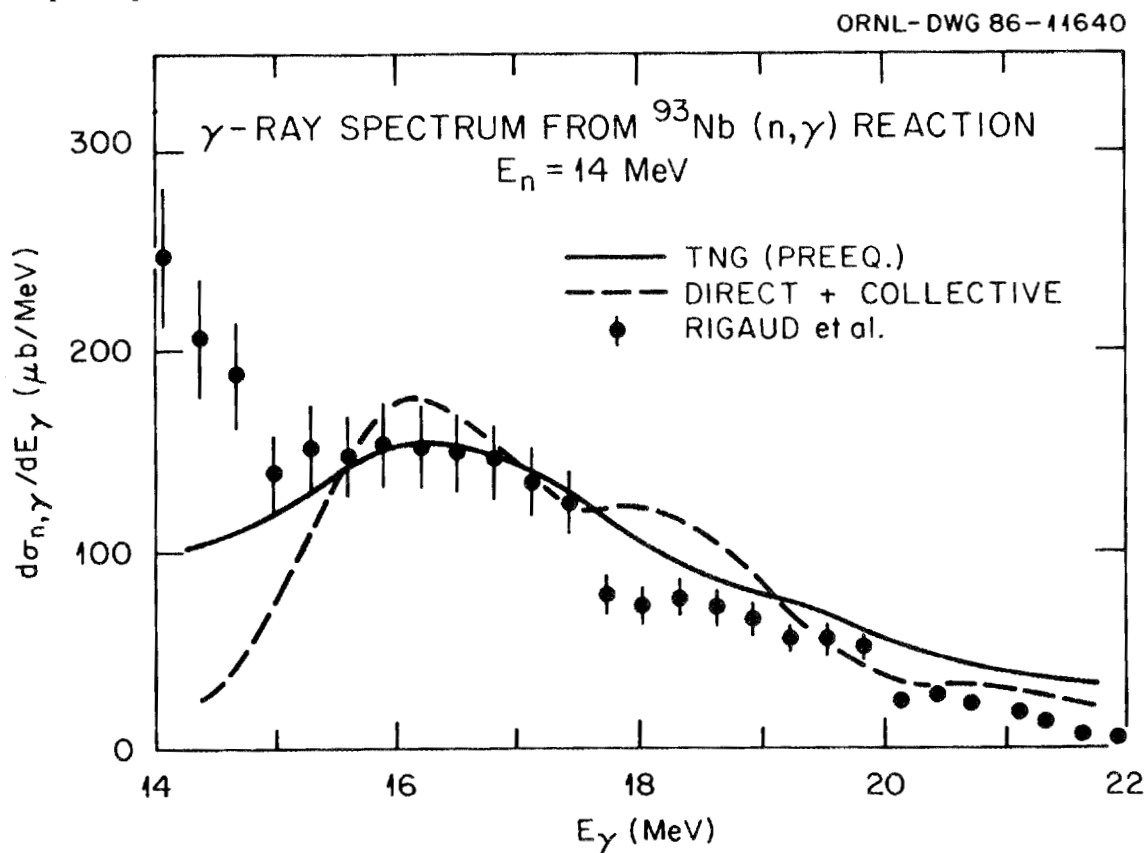


Fig. 5. Gamma-ray spectra emitted from the $^{93}\text{Nb}(n,\gamma)$ reaction at 14.5 MeV. The solid line represents the TNG calculation. The dashed line is the calculation of Rigaud et al. (ref. 8) based on the direct and collective capture models.

where A and B mean the inner and outer barriers, respectively. The quantity $T_A^{J\pi}$ or $T_B^{J\pi}$ is calculated by Eq. (4). When the excitation energy is greater than the inner or outer barrier energy, the fission probability is represented by

$$p_f^{J\pi} = T_f^{J\pi}/T^{J\pi} \quad , \quad (6)$$

where $T^{J\pi}$ is the total transmission coefficient consisting of all possible reaction channels. When the excitation energy is less than both barrier energies, the fission probability is given by¹²

$$P_f^{J\pi} = \left[1 + \left(\frac{T^{J\pi} - T_f^{J\pi}}{T_f^{J\pi}} \right)^2 + 2 \frac{T^{J\pi} - T_f^{J\pi}}{T_f^{J\pi}} \coth \left\{ \frac{1}{2} (T_A^{J\pi} + T_B^{J\pi}) \right\} \right]^{-1/2} \quad (7)$$

In this case, the fission transmission coefficient is renormalized as

$$T_f^{J\pi} = \frac{P_f^{J\pi}}{1 - P_f^{J\pi}} (T^{J\pi} - T_f^{J\pi}) \quad , \quad (8)$$

and thus the total transmission coefficient is also modified.

Concerning the level density for fission transition states, the Gilbert-Cameron's composite formula¹³ used for all other reaction channels can still be used. In general, it is very difficult to determine the parameters for the density of the transition states since no direct measurement of them is possible. Fortunately, Bjornholm and Lynn¹⁴ have compiled the level density parameters for many actinide nuclei. Thus we adopted their values as defaults in TNG. They employed a constant temperature form for the level density, i.e.,

$$\rho(\epsilon, J\pi) = (2J+1) \exp[-(J+\frac{1}{2})^2/2\sigma^2] C e^{\epsilon/\theta} \quad (9)$$

The values of parameters C , θ , and σ recommended by them are listed in Table 2.

We can also calculate multi-chance fission cross sections such as (n, nf) , $(n, 2nf)$, and $(n, 3nf)$. The multi-chance fission is important for the evaluation of actinide nuclei above 5 MeV. As an example, Fig. 6 compares the calculated fission cross sections of ²⁴²Pu with the spread of the available data shown in Ref. 15.

6. SUMMARY

The nuclear model code TNG has been updated. Variable binning for outgoing energies was introduced in order to rectify energy-balance problems. The new binning technique needs no more computer time and has proved to be useful for the evaluation of neutron cross sections.

The new TNG is capable of calculating three additional quantities: capture gamma-ray spectrum, precompound (n, γ) cross section, and fission cross section. The precompound mode of (n, γ) reaction played an important role in reproducing the experimental data above 5 MeV. We have been able to estimate multi-chance fission cross sections, since the fission channels were considered in every reaction step.

**Table 2. Barrier level density parameters
compiled by Bjornholm and Lynn¹⁴**

Type of Nucleus	Range of ϵ (MeV)	Barrier A		Barrier B		σ
		C_A	θ_A	C_B	θ_B	
Even-Even	1.0 - 2.5	0.02135	0.3005			5.7
	2.5 - 2.8	0.0001435	0.1877			6.0
	2.8 - ≥ 5	1.6	0.5			6.3
	1.0 - 1.4			0.02135	0.3005	5.7
	1.4 - 2.0			0.198	0.576	5.7
	2.0 - 3.05			0.00965	0.308	6.0
	3.05 - ≥ 5			0.4265	0.5	6.3
Odd-A	0 - >3	6.8	0.48	3.4	0.48	6.4
Odd-Odd	0 - ~ 2	11.5	0.36	5.75	0.36	6.4
	~ 2 - ≥ 5	54.5	0.5	27.2	0.5	6.4

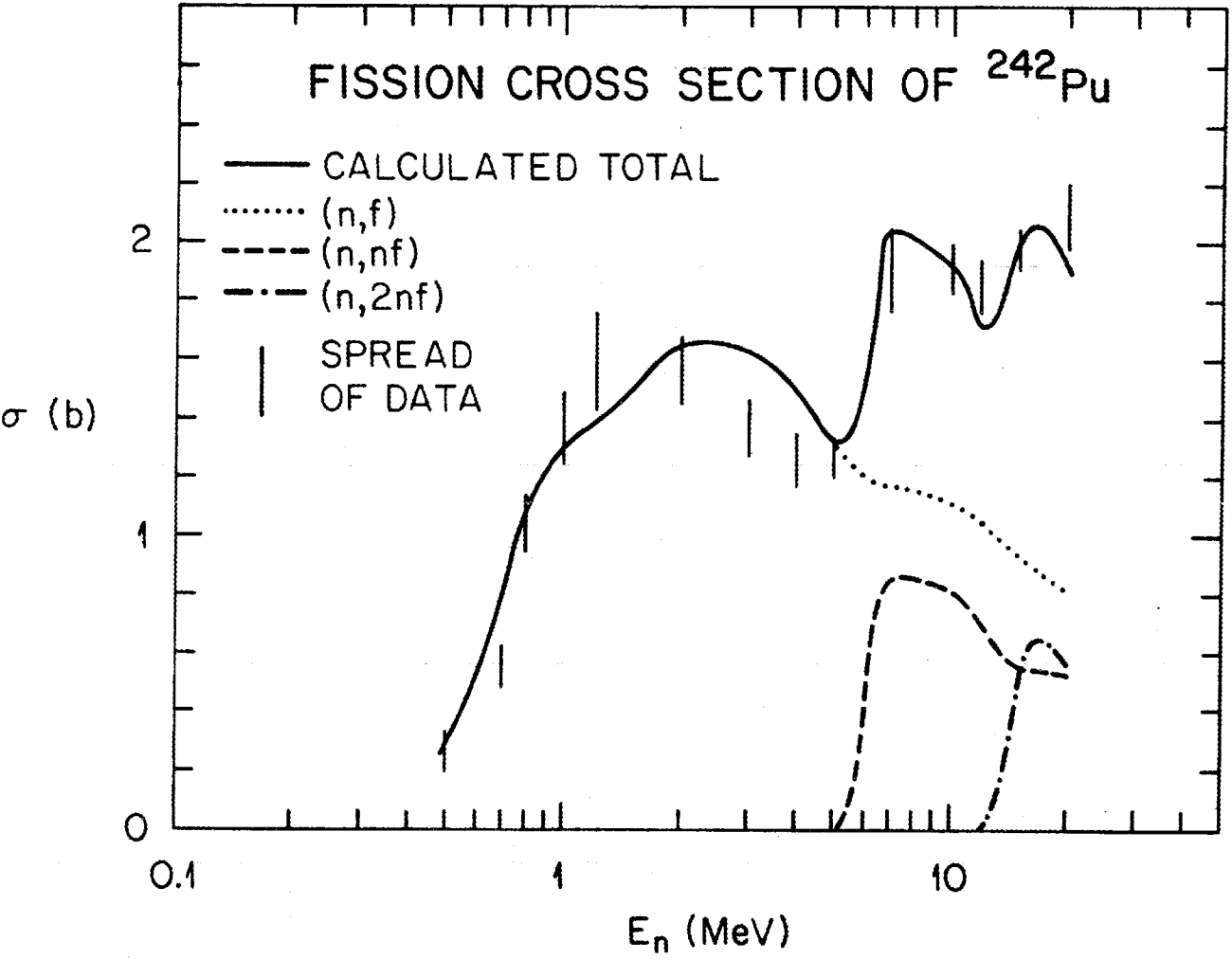


Fig. 6. Calculated fission cross section of ^{242}Pu . The vertical bars represent the spread of the available experimental data (ref. 15).

The work described herein represents positive results of a cooperative effort between Japan and the United States. The extension of the code TNG has been proved and the new version will be used in subsequent evaluation efforts. There are, as might be expected, many new problems to be addressed; for example, inclusion of p -wave data as input to the calculation of gamma-ray production spectra from capture. In addition, angular momentum effects should be considered for the calculation of precompound capture cross sections. And finally, calculation of fission cross sections should include precompound effects.

ACKNOWLEDGEMENTS

One of the authors (K. Shibata) wishes to thank J. K. Dickens, C. Y. Fu, D. M. Hetrick, D. C. Larson, and R. W. Peelle of the Oak Ridge National Laboratory for their hospitality during the course of this work. Helpful comments on the manuscript of this report by J. K. Dickens and D. M. Hetrick are gratefully acknowledged.

REFERENCES

1. C. Y. Fu, *A Consistent Nuclear Model for Compound and Precompound Reactions with Conservation of Angular Momentum*, ORNL/TM-7042 (1980).
2. W. Hauser and H. Feshbach, *Phys. Rev.* **87**, 366 (1952).
3. For example: D. M. Hetrick, C. Y. Fu, and D. C. Larson, *Calculated Neutron-Induced Cross Sections for $^{63,65}\text{Cu}$ from 1 to 20 MeV and Comparisons with Experiments*, ORNL/TM-9083 (1984).
4. C. Y. Fu and D. M. Hetrick, *Update of ENDF/B-V Mod-3 Iron: Neutron-Producing Reaction Cross Sections and Energy-Angle Correlation*, ORNL/TM-9964 (1986).
5. R. E. MacFarlane, Los Alamos National Laboratory, private communication (1985).
6. R. L. Auble, *Nuclear Data Sheets*, **20**, 327 (1977).
7. J. M. Akkermans and H. Gruppelaar, *Phys. Lett.*, **157B**, 95 (1985).
8. F. Rigaud, J. L. Irigaray, G. Y. Petit, G. Longo and F. Saporetti, *Nucl. Phys.*, **A173**, 551 (1971).
9. N. Bohr and J. A. Wheeler, *Phys. Rev.*, **36**, 426 (1939).
10. V. M. Strutinsky, *Nucl. Phys.* **A95**, 420 (1967).
11. D. L. Hill and J. A. Wheeler, *Phys. Rev.*, **89**, 1102 (1953).
12. J. E. Lynn and B. B. Back, *J. Phys.*, **A7**, 395 (1974).
13. A. Gilbert and A. G. W. Cameron, *Can. J. Phys.*, **43**, 1446 (1965).
14. S. Bjornholm and J. E. Lynn, *Rev. Mod. Phys.*, **52**, 725 (1980).
15. D. G. Madland and P. G. Young, *Evaluation of $n + ^{242}\text{Pu}$ Reactions from 10 keV to 20 MeV*, LA-7533-MS (1978).

Appendix A. Explanation of input data for TNG

*****Input read by the MAIN program (Unit 60)*****

Cards 1-3: 3(10A8)

Comments

Card 4: (11I3,5I5)

NBS = Number of binary reactions

= 1 (n,n)
 = 2 (n,n) (n,p)
 = 3 (n,n) (n,p) (n,a)

NE = Number of incident energies

ISTEP1 = Number of integration steps for width
 fluctuation integrals (> 40)

INGMN = Minimum angle of angular distributions
 in deg

INGSP = Angular spacing in deg
 (at most 10 angles allowed)

INGMX = Maximum angle in deg

IPRINT = Printing control
 = 0 Normal output on unit 61
 = 1 Extra debug output

IPCOEF = Printing control
 = 0 No print
 = 1 Print Legendre coefficients in ENDF/B
 format on unit 62

IFLC = Width fluctuation control
 = 0 Do not want it
 = 1 Want it (discrete and continuous levels)

IPCH91 = Printing control
 = 0 No print
 = 1 Print ENDF/B MF = 5, MT = 91 on unit 62
 if ITNG = 0 (see card 15)

ICOMEL = Printing control
 = 0 No print
 = 1 Print compound elastic scattering cross
 sections and Legendre coefficients on
 unit 62 for use in optical-model GENOA

MAT = ENDF/B material number

MT(I) (I=1,NBS) = ENDF/B reaction number for the
I-th reaction

Card 5: (2013)

IOP(I) (I=1,NBS)
 = Optical-model parameter control
 = 1 Read in
 = -1 Neutron Wilmore and Hodgson
 = -2 Neutron Becchetti and Greenlees
 = -3 Proton Becchetti and Greenlees
 = -4 Proton Perey and Perey
 = -5 Alpha Huizenga and Igo
 = -6 Alpha McFadden and Satchler
 = -7 Proton Arthur and Perey
 = -8 Alpha Arthur and Lemo
 = -9 Neutron modified Arthur and Young

JLDIF = Maximum order of Legendre coefficients in
precompound angular distributions (An even
number, 2 recommended for E < 20 MeV)

Card 6: (8011) Skip if IPRINT = 0

IPRT(I) = 1 Print specified quantities listed
(I=1,80) in last part of Appendix A

Card 7: (8011) Skip if JLDIF = 0

IANGL(I) = Continuum angular distribution control for
(I=1,80) the I-th bin
 = 0 Skipped
 = 1 Calculated for compound reaction only
 = 2 Calculated for both compound and
precompound reactions

(NOTE: Continuous bins for different reactions are
stacked. The number of bins with IANGL = 2 should
be less than 8.)

Card 8: (8E10.3)

BN = Binding energy (MeV) of incident particle in
composite system

RAD = Radiative capture control
 = 0.0 No capture
 = 1.0 Want capture (more input in unit 63 with
 NTR = 1; see below)

FISS = Fission control
 = 0.0 No fission
 = 1.0 (n,f)
 = 2.0 (n,f) (n,nf)
 = 3.0 (n,f) (n,nf) (n,2nf)
 and so on

ECENDF = Q-value in MeV of ENDF/B file, section 91
 (will do nothing if set to zero)

YH = Scale factor for precompound angular distribution
 (0.5)

Cards 9-13: Repeated NBS times

Card 9: (6F7.3,A8)

AT = A of residual nucleus
 ZT = Z of residual nucleus
 AI = A of outgoing particle
 ZI = Z of outgoing particle
 Q0 = Q-value for reaction in MeV
 AII = Spin of outgoing particle
 HID = Reaction identification

Card 10: (20I3)

NLVL1 = Number of discrete levels in residual nucleus
 (at most 40)

Card 11: (5(F5.3,F4.1,F4.0,I3))

ENU = Excitation energy of a discrete level in MeV
 AIT = Spin of a discrete level
 AP = Parity of a discrete level
 = -1.0 Negative
 = +1.0 Positive

IDOUT = Printing control
 = 1 Nothing printed
 = 2 Integrated cross sections in mb
 = 3 Angular differential cross sections
 in mb/sr (at most 8 levels can have
 IDOUT = 3)

If IDOUT(1) = 1 or 2, all angular dependent
 calculations are skipped.

Card 12: (7F7.3,I3)

Gilbert-Cameron composite level density parameters

EC = Continuum cut-off E (may be less than any ENU) in
 Mev

EX = Tangency point E in MeV

EO = E in MeV

TM = Constant temperature T in MeV

AC = a in 1/MeV

CC = Spin cut-off parameter c

DELT = Odd-even (pairing) correction U in MeV

ICOUT = Printing cotrol, similar to IDOUT
 = 1 Nothing printed
 = 2 Integrated cross sections in mb
 = 3 Differential cross sections in mb/sr

(NOTE: $c = 0.0888aA^{2/3}$ (Jensen and Luttinger) or
 $c = 0.146aA^{2/3}$ (Facchini and Saetta-Menichella))

Card 13: (8F7.3,2I3/8F7.3) Present if IOP(I) = 1

Optical-model parameters

U = Real well depth in MeV

UE = E-dependence of real potential

RU = Radius of real potential in fm

AU = Diffuseness of real potential in fm

W = Imaginary well depth (surface, volume or Gaussian
 depending on IFS below)

WE = E-dependence of W

RW = Radius of imaginary potential in fm

AW = Diffuseness of imaginary potential in fm

IFS = 1 Woods-Saxon surface
 = 0 Woods-Saxon volume
 = -1 Gauss

ISTEP = Number of steps used in optical-model
 calculations (40)

WV = Volume part of imaginary well depth in MeV
 (additional to W if IFS = 1)

WVE = E-dependence of WV

UEE = E**2 dependence of real potential in 1/MeV

RC = Coulomb radius in fm

(The real potential is assumed to have Woods-Saxon
 form factor. E is the laboratory energy.)

Card 14: (2F7.0,E7.1,6F7.0)

ACC = Level density parameter 'a' for composite system
 in 1/MeV

QC = Pairing correction for composite system in MeV

TCUT = Transmission coefficient cut-off

FA = Clustering probability for alpha (0.1 - 0.2)

FG = Scale factor for precompound mode of (n,gamma)
 reaction (1.0)

F2 = Scale factor for M**3 (4.0 - 7.0)

TIME = cutoff time in arbitrary units set internally
 for integration of master equation (1000.0)

FP = Scale factor for precompound mode of (n,p)
 reaction (1.0)

CCSIG = Mean-square of magnetic quantum number for
 single particle states ($\langle m \rangle = \text{CCSIG} \cdot A^{2/3}$)
 = 0.146 Jensen and Luttinger
 = 0.240 Facchini and Saetta-Menichella

Card 15: (3I5,7E10.0)

There are NE cards, each for one energy.

ISDI = 0 No direct interaction cross-section input
 = 1 There is direct-interaction cross-section
 input for discrete levels (needed only for
 gamma-ray production calculations).

(NOTE: If ISDI =1, effects of direct interaction are
 included automatically and should not be included again
 in OTHER below.)

ITNG = 0 Single step (binary) calculation
 = 1 Multistep calculations

IPRE = 0 No precompound calculation
 = 1 Precompound calculation desired ($E > 5$ MeV)

E = Incident particle energy, laboratory (MeV)

DBIN = Bin width (MeV) for outgoing particle energies
 and continuum, must be such that the number of
 bins per nucleus is at most 40. If negative,
 variable bin widths are used (additional input
 on cards 16 -17). If zero, the code uses the
 same bins as in the previous energy run.

EGBIN = Bin width for emitted gamma-ray energies in MeV

OTHER = Cross section in mb for reactions not included
 in the calculation for normalization.

GGAM = S-wave radiative width (ev) for energy E

GCRM = Normalization factor. If RAD = 1.0 (see card 8)
 and GGAM = 0.0, calculated radiative width is
 multiplied by GCRM.

Cards 16-17: 2(20F4.1) Skip if DBIN is not negative.

BINI(I) (I = 1,40) = Variable bin widths in MeV

Cards 18-19: Repeated NBS times if ISDI = 1

Card 18: (I5)

NSDI = Number of levels for which direct-interaction cross sections are to be put in for the I-th residual nucleus

Card 19: (I5,E10.4)

There are NSDI pairs of NXW and SDI.

NXW = Level number of current residual nucleus
(NXW = -1 for ground state)

SDI = Direct-interaction cross section in mb for the NXW-th level

*****Input read by INPUT and TNG subroutines (Unit 63)*****

Cards 1-17: Repeated NBS times if both RAD and FISS are equal to 0.0.
Repeated (NBS + 1) times if either RAD or FISS is not equal to 0.0.

Card 1: (16I5)

MAT = ENDF/B material number

NTR = Number of tertiary reactions (NOTE: Fission reactions should not be included in NTR.)

IPCHN = Printing control for particle production cross sections
= 0 Do not print
= 1 Print

IPCHG = Printing control for gamma-ray production cross sections
= 0 Do not print
= 1 Print

Card 2: (8F10.0)

EMRAT = Fraction of M1 strength at 7 MeV relative to E1

EERAT = E2/E1 assuming same energy dependence for transmission coefficients

Cards 3-11: Repeated NTR times

Card 3: (A4)

TITLE = Title, such as n,np

Gamma-ray channels such as (n,n gamma) must come first.

CARD 4: (16I5)

NLEV = Number of discrete levels of residual nucleus
for the I-th reaction

NTPCRD = Number of cards containing gamma-ray branching
ratios
= 0 if gamma-ray production not wanted

(NOTE: One should be careful not to double count the
gamma-rays from a given reaction. For example, the
gamma-ray production from (n,2n) can be included in
either the 2nd step or the 3rd step but should not
be in both.)

N1 = Index for tallying particle y in (x,yz) reaction
for total particle production cross sections
= 0 Do not tally
= 1 Tally it as a neutron
= 2 Tally it as a proton
= 3 Tally it as an alpha

N2 = Index for tallying particle z in (x,yz) reaction
for total particle production cross sections

MT = Reaction number in ENDF/B format

NNUC = 1 Read in optical-model parameters
= -1 Neutron Wilmore and Hodgson
= -2 Neutron Becchetti and Greenlees
= -3 Proton Becchetti and Greenlees
= -4 Proton Perey and Perey
= -5 Alpha Huizenga and Igo
= -6 Alpha McFadden and Satchler
= -7 Proton Arthur and Perey
= -8 Alpha Arthur and Lemo
= -9 Neutron modified Arthur and Young

NGAM = 1 giant dipole parameters read in card 9
= 0 Use defaults

NCAP = Number of cards containing primary gamma-ray
branching ratios read in card 11
= 0 The code calculates the branching ratios

(NOTE: NCAP is needed only for (n,gamma) reaction.
Otherwise, it should be set to 0.)

Card 5: (8F10.0)

AT1 = Mass of residual nucleus

AI1 = Mass of outgoing particle

ZT1 = Charge of residual nucleus

ZI1 = Charge of outgoing particle

SI1 = Spin of outgoing particle (0.0 for gamma-rays)

Q2 = Q-value in MeV

Card 6: (5(F5.3,F4.1,F4.0,3X))

There are NLEV discrete levels.

ELEV = Excitation energy (MeV)

SPIN = Spin

PAR = Parity

Card 7: (8(2I3,F4.2)) Skip if NTPCRD = 0

L = Index for initial level of gamma-ray transition

M = Level number for final level (1 for ground state)

BR = Branching ratio for transition from L to M
 = 2.0 0+ to 0+ transition (0.51-MeV gamma rays)
 = 3.0 Isomeric state L (M = L - 1)

(NOTE: L, M, BR sets for BR = 0 need not be put in.
 Unless BR = 2. or 3., sum of BR over M should be 1.)

Card 8: (8F7.0,2I3/8F7.0) Present if NNUC =1, skip if
 (n,gamma), (n,n gamma), etc.

U = Real well depth in MeV

UE = E-dependence of real potential

RU = Radius of real potential in fm

AU = Diffuseness of real potential in fm

W = Imaginary well depth in MeV (surface, volume or
 Gaussian depending on IFS below)

WE = E-dependence of imaginary potential

RW = Radius of imaginary potential in fm

AW = Diffuseness of imaginary potential in fm

IFS = 1 Woods-Saxon surface
 = 0 Woods-Saxon volume
 = -1 Gauss

ISTEP = Number of steps used in optical-model
 calculations (40)

WV = Volume part of imaginary depth in MeV (additional
 to W if IFS =1)

WVE = E-dependence of WV

UEE = E**2-dependence of real potential in 1/MeV

RC = Coulomb radius in fm

(NOTE: The real potential is assumed to have Woods
 -Saxon form factor. E is the laboratory energy.)

Card 9: (8F10.0) Present if NGAM = 1

Giant dipole resonance parameters (Lorentzian form)

E1 = Resonance energy in MeV

GAM1 = Full width at half maximum in MeV

SIG1 = Peak cross section in mb

GSTEP = Energy below which GDR cross section is
 multiplied by GFRAC

GFRAC = Factor referred to above

E2 = Energy for the second resonance in MeV (=0 if
 single peak)

GAM2 = Full width at half maximum for the second
 resonance

SIG2 = Peak cross section for the second resonance

Card 10: (7F7.0)

Level density parameters

EC = Continuum cut-off E in MeV

EX = Tangency point E in MeV

EO = E in MeV

TM = Constant temperature T in MeV

AC = a in 1/MeV

CC = Spin cut-off factor c

DELC = Odd-even pairing correction U in MeV

Card 11: (10(I3,F5.0)) Skip if NCAP = 0

There must be NCAP cards.

MC = Level number for final state

BRC = Branching ratio for primary transition to MC

(NOTE: If sum of BRC over MC is less than 1.0, the code combines the input BRC's with calculated ones.)

Cards 12-16: Present if you want to calculate fission cross sections in this step.

Card 12: (A4,I5)

TITLF = Reaction identification such as (n,f)

MTF = Reaction number in ENDF/B format

Card 13: (8F10.0)

Parameters for the double-humped barrier model

EB(1) = Inner barrier height in MeV

EB(2) = Outer barrier height in MeV

HOM(1) = Inner barrier curvature in MeV

HOM(2) = Outer barrier curvature in MeV

(NOTE: If EB(2) = 0.0, the single-humped barrier model is employed.)

Cards 14-16: Repeated twice if the double-humped barrier model adopted

Card 14: (16I5)

NLEVF = Number of discrete levels at a barrier

Card 15: (5(F5.3,F4.1,F4.0,3X))

ELEVF = Excitation energy in MeV relative to the
barrier.

SPINF = Spin of the level

PARF = Parity of the level
= -1.0 Negative
= +1.0 Positive

Card 16: (8F7.0)

Level density parameters for transition states

ECF = Continuum cut-off E in MeV

EXF = Tangency point E in MeV

EOF = E in MeV

TMF = Constant temperature T in MeV

ACF = a in 1/MeV

CCF = Spin cut-off factor c

DELFCF = Pairing correction U in MeV

(NOTE: If TMF and ACF are equal to 0.0, default
level density recommended by Lynn is used.)

Card 17: (5I5) Skip if (n,gamma) or (n,f)

IA = Reaction index in previous step from which to
branch into current step

= 1 (n,n)

= 2 (n,p)

= 3 (n,a)

IMORE = 0 Return to previous step
= 1 More reaction to be done in current step
or, if ISTORE = 1, go to next step

ISTORE = 0 Do not store current output for next step
= 1 Store current output

*****Details of card 6 on unit 60*****

IPRT(I) = 1 Print the specified quantities
= 0 Do not print

- I = 1: Transmission coefficients for incident neutron and outgoing particles exciting the continuum bins
- in TRANS subroutine
- 2: Giant dipole cross section - INPUT
- 3: Level density integrated over each bin - INPUT
- 4: Gamma-ray transmission coefficients in capture
- COMPET
- 5: Gamma-ray transmission coefficients, radiative widths, and width-fluctuation corrections for capture and continuum - HOWZT
- 6: Iteration for conversion to single-fermion level-density parameters - DNCONV
- 7: Details of pairing correction - PAIR
- 8: Spin distribution in formation and 2p-1h states
- DNTRN
- 9: Inverse reaction cross sections - PRECOA
- 10: Transmission coefficients in 2nd and 3rd steps
- TRANS1
- 11: Continuum spin and parity distributions in 2nd and 3rd steps - NORM
- 12: Partial gamma-ray production from each spin and parity of continuum states if $> 10\text{mb}$ - CASCAD
- 13: Spin weights (SWT) of levels in 2nd and 3rd steps if $IC = 1$, i.e., 1st bin in (n,n gamma) - COMPET
- 14: Legendre coefficients for each spin and parity of continuum bins with $IANGL = 2$ - HOWZT

- 15: Details in angular momentum coupling - HOWZT
- 16: Details of precompound calculations - PRECOA (saved in unit 64 even if IPRT(16)=0)
- 17: More details of precompound calculations - OMEFF (saved in unit 64 even if IPRT(17)=0)
- 18: Gamma-ray production cross sections and energy distributions for individual reactions - CASCAD
- 19: First-chance fission transmission coefficients - INPUT
- 20: Continuum transmission coefficients for fission - TRFISS

Appendix B. INPUT DATA FOR SAMPLE CALCULATIONS

***** SAMPLE 1. FE-56(N,XN) AND FE-56(N,XP) *****

***** INPUT ON UNIT 60 *****

IRON-56 ** VARIABLE BINNING **
 GILBERT AND CAMERON DENSITIES WITH CC=0.0888*AC*AT**(2/3)
 GLOBAL OPTICAL MODEL PARAMETERS BY DEFAULT

```

3 1 20 00 10 90 1 1 1
-9 -3 -5
00 00 0
7.700 4.5390
56. 26. 1. 0. 0. .5 (N,N)
26
0000 00 +1 2 0847 20 +1 2 2085 40 +1 2 2658 20 +1 2 2942 00 +1 2
2960 20 +1 2 3120 10 +1 2 3123 40 +1 2 3370 20 +1 2 3388 60 +1 2
3445 30 +1 2 3449 10 +1 2 3602 20 +1 2 3607 00 +1 2 3756 60 +1 2
3832 20 +1 2 3857 30 +1 2 4049 30 +1 2 4100 30 +1 2 4120 40 +1 2
4298 40 +1 2 4302 00 +1 2 4395 30 +1 2 4401 20 +1 2 4458 40 +1 2
4510 30 -1 2
4.539 10.75 -.1050 1.417 6.355 8.2600 2.81 2
56. 25. 1. 1. -2.913 .5 (N,P)
10
0000 30 +1 2 0026 20 +1 2 0111 10 +1 2 0212 40 +1 2 0215 20 +1 2
0335 50 +1 2 0341 30 +1 2 0454 40 +1 2 0486 30 +1 2 0716 30 +1 2
0.754 7.676 -2.200 1.256 7.233 9.401 .525 2
53. 24. 4. 2. .247 0. (N,A)
14
0000 15 -1 2 0564 05 -1 2 1006 25 -1 2 1290 35 -1 2 1537 35 -1 2
1974 25 -1 2 2172 55 -1 2 2233 45 -1 2 2321 15 -1 2 2453 35 -1 2
2657 25 -1 2 2671 05 -1 2 2706 55 -1 2 2708 15 -1 2
2.681 7.673 -.7622 1.288 6.500 8.144 1.35 2
6.923 1.540 1.0E-07 0.2 1.0 4.0 3000. 1. 0.2
1 1 1 14.5 -1. .025 0.00 0.0 1.0
  
```

.025.050.075.100.125.150.175.200.225.250.275.300.325.350.375.400.425.450.475.500
 .525.550.575.600.625.650.675.700.725.750.775.800.825.850.875.900.925.950.9751.00

14
 2 73.1
 3 0.75
 4 4.90
 6 0.53
 8 5.90
 9 4.63
 10 0.68
 13 3.15
 15 0.76
 16 1.11
 20 1.45
 21 1.15
 24 2.91
 26 7.35

***** INPUT ON UNIT 63 *****

2656 2 1 1
 0.1 0.01

N,PG

10 3 2 0 103
 56.0 0.0 25.0 0.0 0.0 -2.913
 0000 30 +1 2 0026 20 +1 2 0111 10 +1 2 0212 40 +1 2 0215 20 +1 2
 0335 50 +1 2 0341 30 +1 2 0454 40 +1 2 0486 30 +1 2 0716 30 +1 2
 2 1 1.0 3 1 .01 3 2 .99 4 1 1.0 5 1 .08 5 2 .16 5 3 .76 6 1 .72
 6 4 .28 7 4 .70 7 5 .30 8 1 .89 8 4 .02 8 6 .07 8 7 .02 9 1 .02
 9 2 .20 9 4 .06 9 5 .71 9 7 .01 10 1 .38 10 7 .43 10 9 .19
 0.754 7.676 -2.200 1.256 7.233 9.401 .525 2

N,PN

16 4 2 1 28 -9
 55.0 1.0 25.0 0.0 0.5 -10.18

0000	25	-1	2	0126	35	-1	2	0984	45	-1	2	1292	55	-1	2	1528	15	-1	2				
1884	35	-1	2	2015	35	-1	2	2198	35	-1	2	2215	25	-1	2	2252	15	-1	2				
2267	25	-1	2	2312	65	-1	2	2366	25	-1	2	2398	35	-1	2	2427	05	+1	2				
2563	15	-1	2																				
2	1	1.0	3	1	.05	3	2	.95	4	2	.80	4	3	.20	5	1	.97	5	2	.03	6	1	.57
6	2	.43	7	1	.08	7	3	.92	8	1	.61	8	2	.06	8	3	.33	9	1	1.0	10	1	1.0
11	1	.72	11	5	.28	12	3	.10	12	4	.90	13	1	.26	13	2	.74	14	2	.75	14	3	.25
15	1	1.0	16	1	1.0																		
2.570	7.920	-1.045	1.289	6.665	8.560	1.27																	
2	1																						
2656	2	1	1																				

0.1 0.01

N,AG

14	3	3	0	107																			
53.0		0.0		24.0		0.0		0.0		0.247													
0000	15	-1	2	0564	05	-1	2	1006	25	-1	2	1290	35	-1	2	1537	35	-1	2				
1974	25	-1	2	2172	55	-1	2	2233	45	-1	2	2321	15	-1	2	2453	35	-1	2				
2657	25	-1	2	2671	05	-1	2	2706	55	-1	2	2708	15	-1	2								
2	1	1.0	3	1	1.0	4	1	.93	4	3	.07	5	1	.09	5	3	.65	5	4	.26	6	1	.84
6	4	.16	7	4	1.0	8	5	1.0	9	1	1.0	10	3	.60	10	4	.40	11	1	.05	11	3	.68
11	4	.27	12	1	1.0	13	7	1.0	14	1	.11	14	2	.44	14	3	.28	14	6	.13	14	9	.04
2.681	7.673	-.7622	1.288	6.500	8.144	1.35	2																

N,AN

12	3	3	1	22	-9																		
52.0		1.0		24.0		0.0		0.5		-7.61													
0000	00	+1	2	1434	20	+1	2	2370	40	+1	2	2647	00	+1	2	2768	40	+1	2				
2965	20	+1	2	3114	60	+1	2	3162	20	+1	2	3415	40	+1	2	3472	30	+1	2				
3616	50	+1	2	3772	20	+1	2																
2	1	1.0	3	2	1.0	4	2	1.0	5	2	.99	5	3	.01	6	2	1.0	7	3	.99	7	5	.01
8	1	.13	8	2	.87	9	2	.07	9	3	.14	9	5	.79	10	2	.22	10	5	.78	11	3	.54
11	5	.42	11	7	.03	11	9	.01	12	1	.20	12	2	.80									
3.700	9.7940	-.1830	1.392	6.154	7.613	2.65	2																
3	1																						
2656	4	1	1																				

0.1 0.01


```

0000 25 -1 2 0126 35 -1 2 0984 45 -1 2 1292 55 -1 2 1528 15 -1 2
1884 35 -1 2 2015 35 -1 2 2198 35 -1 2 2215 25 -1 2 2252 15 -1 2
2267 25 -1 2 2312 65 -1 2 2366 25 -1 2 2398 35 -1 2 2427 05 +1 2
2563 15 -1 2
  2 1 1.0 3 1 .05 3 2 .95 4 2 .80 4 3 .20 5 1 .97 5 2 .03 6 1 .57
  6 2 .43 7 1 .08 7 3 .92 8 1 .61 8 2 .06 8 3 .33 9 1 1.0 10 1 1.0
11 1 .72 11 5 .28 12 3 .10 12 4 .90 13 1 .26 13 2 .74 14 2 .75 14 3 .25
15 1 1.0 16 1 1.0
2.570 7.920 -1.045 1.289 6.665 8.560 1.27

```

N,NA

```

  12 3 1 3 22 -5
  52.0 4.0 24.0 2.0 0.0 -7.61
0000 00 +1 2 1434 20 +1 2 2370 40 +1 2 2647 00 +1 2 2768 40 +1 2
2965 20 +1 2 3114 60 +1 2 3162 20 +1 2 3415 40 +1 2 3472 30 +1 2
3616 50 +1 2 3772 20 +1 2
  2 1 1.0 3 2 1.0 4 2 1.0 5 2 .99 5 3 .01 6 2 1.0 7 3 .99 7 5 .01
  8 1 .13 8 2 .87 9 2 .07 9 3 .14 9 5 .79 10 2 .22 10 5 .78 11 3 .54
11 5 .42 11 7 .03 11 9 .01 12 1 .20 12 2 .80
3.700 9.7940 -.1830 1.392 6.154 7.613 2.65 2
  1

```

***** SAMPLE 2. FE-56(N,GAMMA) GAMMA-RAY SPECTRUM *****
*

***** INPUT ON UNIT 60 *****

IRON-56 ** CAPTURE GAMMA-RAY SPECTRUM **
GILBERT AND CAMERON DENSITIES WITH CC=0.0888*AC*AT**(2/3)
GLOBAL OPTICAL MODEL PARAMETERS BY DEFAULT

```

1 1 20 00 10 90 1 1 1
-9
00 00 0 1
7.700 1.0 4.5390
56. 26. 1. 0. 0. .5 (N,N)
26

```

```

0000 00 +1 2 0847 20 +1 2 2085 40 +1 2 2658 20 +1 2 2942 00 +1 2
2960 20 +1 2 3120 10 +1 2 3123 40 +1 2 3370 20 +1 2 3388 60 +1 2
3445 30 +1 2 3449 10 +1 2 3602 20 +1 2 3607 00 +1 2 3756 60 +1 2
3832 20 +1 2 3857 30 +1 2 4049 30 +1 2 4100 30 +1 2 4120 40 +1 2
4298 40 +1 2 4302 00 +1 2 4395 30 +1 2 4401 20 +1 2 4458 40 +1 2
4510 30 -1 2
4.539 10.75 -.1050 1.417 6.355 8.2600 2.81 2
6.923 1.540 1.0E-07 0.2 1.0 4.0 3000. 1. 0.2
0 0 0 0.10 0.5 .250 0.00 0.0 1.0

```

***** INPUT ON UNIT 63 *****

```

2656 1 1 1
0.1 0.01
N,G
20 5 0 0 102 0 0 1
57.0 0.0 26.0 0.0 0.0 7.6466
0000 05 -1 2 0014 15 -1 2 0137 25 -1 2 0367 15 -1 2 0706 25 -1 2
1007 35 -1 2 1198 45 -1 2 1265 05 -1 2 1366 35 -1 2 1628 15 -1 2
1726 15 -1 2 1975 05 -1 2 1989 45 -1 2 2117 25 -1 2 2207 25 -1 2
2219 15 -1 2 2335 05 -1 2 2355 55 -1 2 2455 45 +1 2 2506 25 +1 2
2 1 1.0 3 1 .12 3 2 .88 4 1 .11 4 2 .78 4 3 .11 5 1 .04 5 2 .85
5 3 .08 5 4 .03 6 2 .36 6 3 .64 7 3 1.0 8 2 .11 8 4 .89 9 5 1.0
10 2 .64 10 4 .28 10 5 .08 11 1 .54 11 4 .13 11 5 .16 11 6 .17 12 2 1.0
13 7 1.0 14 2 1.0 15 2 1.0 16 1 1.0 17 2 1.0 18 6 0.7 18 7 0.3 19 6 1.0
20 4 1.0
2.56 9.862 -1.587 1.366 6.923 9.023 1.54 2
1 .221 2 .272 4 .046 8.0064 10 .081 11 .083 14 .002

```

***** SAMPLE 3. NB-93(N,GAMMA) PRECOMPOUND CROSS SECTION *****

***** INPUT ON UNIT 60 *****

NIOBIUM-93 PRECOMPOUND CAPTURE
GILBERT AND CAMERON DENSITIES WITH $CC=0.1460*AC*AT^{2/3}$
GLOBAL OPTICAL MODEL PARAMETERS BY DEFAULT

```
3 1 20 00 30180 0 0 1
1 -4 -5
7.229 1.0 0.0 0.0 0.55
93.0 41.0 1.0 0.0 0.0 0.5 (N,N)
14
0000 45 +1 2 0030 05 -1 2 0686 15 -1 2 0744 35 +1 2 0809 25 +1 2
0810 15 -1 2 0950 65 +1 2 0979 55 +1 2 1083 45 +1 2 1127 25 +1 2
1290 15 -1 2 1297 45 +1 2 1316 15 -1 2 1335 85 +1 2
1.364 4.931 -.5593 0.729 12.580 37.68 0.72 2
48.000 -.293 1.270 0.660 9.600 .000 1.270 .470 1 40
93.0 40.0 1.0 1.0 0.690 0.5 (N,P)
13
0000 25 +1 2 0267 15 +1 2 0947 05 +1 2 1018 05 +1 2 1151 05 +1 2
1222 05 +1 2 1426 15 +1 2 1436 05 +1 2 1450 15 +1 2 1470 25 +1 2
1477 35 +1 2 1597 25 +1 2 1648 15 +1 2
1.735 5.208 .1712 .7117 12.690 38.00 1.20 2
90.0 39.0 4.0 2.0 4.918 0.0 (N,A)
10
0000 20 -1 2 0203 30 -1 2 0682 70 +1 2 0777 20 +1 2 0954 30 +1 2
1047 50 +1 2 1190 40 +1 2 1215 00 -1 2 1298 60 +1 2 1371 10 -1 2
1.417 3.546 -0.505 .8347 10.260 27.30 .327 2
12.510 0.0 1.0E-07 0.2 1.0 4.5 3000. 1.0 .24
0 1 1 14.000 0.5 0.250 000.0 0.0 1.0
```

***** INPUT ON UNIT 63 *****

```
4193 1 1 1
0.1 0.01
```

N,G

8 0 0 0 0 0 1
 94.0 0.0 41.0 0.0 0.0 7.229
 0000 60 +1 2 0041 30 +1 2 0059 40 +1 2 0079 70 +1 2 0118 50 +1 2
 0140 20 -1 2 0312 50 +1 2 0334 20 +1 2
 16.5 5.0 162.
 0.396 4.097 -1.109 .724 12.51 37.735 0.0
 4193 2 1 1
 0.1 0.01

N,PG

13 2 2 0 103 0 1
 93.0 0.0 40.0 0.0 0.0 0.690
 0000 25 +1 2 0267 15 +1 2 0947 05 +1 2 1018 05 +1 2 1151 05 +1 2
 1222 05 +1 2 1426 15 +1 2 1436 05 +1 2 1450 15 +1 2 1470 25 +1 2
 1477 35 +1 2 1597 25 +1 2 1648 15 +1 2
 2 1 1.0 3 1 .76 3 2 .24 4 2 1.0 5 2 1.0 6 2 1.0 7 1 .90 7 2 .10
 8 2 1.0 9 1 .89 9 2 .11 10 1 .40 10 2 .60 11 1 1.0 12 2 1.0 13 1 1.0
 16.5 5.0 162.
 1.735 5.208 .1712 .7117 12.690 38.00 1.20 2

N,PN

9 2 2 1 28 1 1
 92.0 1.0 40.0 0.0 0.5 -6.042
 0000 00 +1 2 0934 20 +1 2 1383 00 +1 2 1495 40 +1 2 1847 20 +1 2
 2067 20 +1 2 2150 40 +1 2 2340 30 -1 2 2398 40 +1 2
 2 1 1.0 3 2 1.0 4 1 1.0 5 1 .36 5 2 .64 6 2 1.0 7 4 1.0 8 1 .01
 8 2 .73 8 4 .19 8 5 .07 9 4 1.0
 48.000 -.293 1.270 0.660 9.600 .000 1.270 .470 1 40

16.5 5.0 162.
 2.486 6.052 .8327 .7524 11.830 35.17 1.92 2
 2 1
 4193 2 1 1
 0.1 0.01

N,AG

10 2 3 0 107 0 1
 90.0 0.0 39.0 0.0 0.0 4.918

0000 20 -1 2 0203 30 -1 2 0682 70 +1 2 0777 20 +1 2 0954 30 +1 2
 1047 50 +1 2 1190 40 +1 2 1215 00 -1 2 1298 60 +1 2 1371 10 -1 2
 2 1 1.0 3 2 1.0 4 1 .78 4 2 .22 5 1 .42 5 4 .58 6 3 1.0 7 5 .89
 7 6 .11 8 1 1.0 9 3 .95 9 6 .05 10 1 1.0

16.5 5.0 162.
 1.417 3.546 -0.505 .8347 9.3180 27.30 0.0 2

N,AN

3 1 3 1 22 1 1
 89.0 1.0 39.0 0.0 0.5 -1.939
 0000 05 -1 2 0909 45 +1 2 1507 15 -1 2
 2 1 1.0 3 1 1.0
 48.000 -.293 1.270 0.660 9.600 .000 1.270 .470 1 40

16.5 5.0 162.
 1.745 3.557 .8578 .8075 8.600 25.01 0.93

3 1
 4193 4 1 1
 0.1 0.01

N,NG

14 3 1 0 91 0 1
 93.0 0.0 41.0 0.0 0.0 0.0
 0000 45 +1 2 0030 05 -1 2 0686 15 -1 2 0744 35 +1 2 0809 25 +1 2
 0810 15 -1 2 0950 65 +1 2 0979 55 +1 2 1083 45 +1 2 1127 25 +1 2
 1290 15 -1 2 1297 45 +1 2 1316 15 -1 2 1335 85 +1 2
 2 1 3.0 3 2 1.0 4 1 1.0 5 1 .99 5 4 .01 6 2 1.0 7 2 1.0 8 1 1.0
 9 1 .27 9 4 .66 9 8 .07 10 5 1.0 11 3 1.0 12 1 .53 12 4 .30 12 8 .17
 13 4 1.0 14 7 1.0

16.5 5.0 162.
 1.364 4.931 -.5593 0.729 12.580 37.68 0.72 2

N,2N

7 2 1 1 16 1 1
 92.0 1.0 41.0 0.0 0.5 -8.832
 0000 70 +1 2 0136 20 +1 2 0226 20 -1 2 0286 30 +1 2 0357 50 +1 2
 0390 30 -1 2 0480 40 +1 2
 2 1 3.0 3 2 1.0 4 2 1.0 5 1 1.0 6 2 .03 6 3 .96 6 4 .01 7 4 .76
 7 5 .24

48.000 -.293 1.270 0.660 9.600 .000 1.270 .470 1 40

16.5 5.0 162.
0.501 4.299 -1.122 .8341 10.300 30.63 0.0

N,NP

9 2 1 2 28 -4 1
92.0 1.0 40.0 1.0 0.5 -6.042
0000 00 +1 2 0934 20 +1 2 1383 00 +1 2 1495 40 +1 2 1847 20 +1 2
2067 20 +1 2 2150 40 +1 2 2340 30 -1 2 2398 40 +1 2
2 1 1.0 3 2 1.0 4 2 1.0 5 1 .36 5 2 .64 6 2 1.0 7 4 1.0 8 1 .01
8 2 .73 8 4 .19 8 5 .07 9 4 1.0
16.5 5.0 162.
2.486 6.052 .8327 .7524 11.830 35.17 1.92 2

N,NA

3 1 1 3 22 -5 1
89.0 4.0 39.0 2.0 0.0 -1.939
0000 05 -1 2 0909 45 +1 2 1507 15 -1 2
2 1 1.0 3 1 1.0
16.5 5.0 162.
1.745 3.557 .8578 .8075 8.600 25.01 0.93
1 1 1
4193 2 1 1
0.1 0.01

N2NG

7 2 0 0 4 0 1
92.0 0.0 41.0 0.0 0.0 -8.832
0000 70 +1 2 0136 20 +1 2 0226 20 -1 2 0286 30 +1 2 0357 50 +1 2
0390 30 -1 2 0480 40 +1 2
2 1 3.0 3 2 1.0 4 2 1.0 5 1 1.0 6 2 .03 6 3 .96 6 4 .01 7 4 .76
7 5 .24
16.5 5.0 162.
0.501 4.299 -1.122 .8341 10.300 30.63 0.0

N,3N

13 2 0 1 17 1 1
91.0 1.0 41.0 0.0 0.5 -16.715

0000 45 +1 2 0105 05 -1 2 1187 25 -1 2 1313 15 -1 2 1581 35 +1 2
 1613 15 -1 2 1637 45 +1 2 1790 45 -1 2 1845 25 -1 2 1885 05 +1 2
 1963 25 +1 2 1984 65 -1 2 2035 85 -1 2
 2 1 1.0 3 2 1.0 4 2 1.0 5 1 1.0 6 2 .99 6 3 .01 7 1 1.0 8 1 1.0
 9 2 1.0 10 2 1.0 11 1 1.0 12 1 .51 12 8 .49 13 12 1.0
 48.000 -.293 1.270 0.660 9.600 .000 1.270 .470 1 40

16.5 5.0 162.
 2.065 5.609 -.2735 .9117 9.4000 27.75 0.93 2
 1 0 0

***** SAMPLE 4. PU-242 FISSION CROSS SECTION *****

***** INPUT ON UNIT 60 *****

N + PU-242 FISSION TEST CASE
 MOST OF PARAMETERS TAKEN FROM MADLAND-YOUNG
 BARRIER PARAMETERS TAKEN FROM BJORNHOLM-LYNN

1 21 20 0 20 90 1 0 1 0 0
 1

1
 5.0342 1.0 3.0 0.0 0.55
 242.0 94.0 1.0 0.0 0.0 0.5 (N,N)

20
 0000 00 +1 2 0044 20 +1 2 0147 40 +1 2 0306 60 +1 2 0518 80 +1 2
 0779 100 +1 2 0780 10 -1 2 0833 30 -1 2 0865 30 -1 2 0927 50 -1 2
 0956 00 +1 2 0986 20 -1 2 0995 20 +1 2 1019 30 -1 2 1040 40 +1 2
 1064 40 -1 2 1087 120 +1 2 1102 20 +1 2 1122 50 -1 2 1152 20 -1 2
 1.152 4.035 -0.015 0.390 27.797 94.99 1.100 2
 47.626 -0.344 1.203 0.628 5.913 -0.255 1.306 0.57 1 40
 -0.566 0.210
 27.623 0.710 1.0E-7 0.2 1.0 4.5 3000.0 1.0 0.146
 0 0 0 0.500 -1.0 1.0 000. 0.0 0.2
 0.2 0.2 0.2 0.2 0.2 0.2 0.2 0.2 0.2 0.3 0.4 0.6 0.8 1.0 1.0 1.0 1.0 1.0 1.0 1.0
 1.0 1.0 1.0 1.0 1.0 1.0 1.0 1.0 1.0 1.0 1.0 1.0 1.0 1.0 1.0 1.0 1.0 1.0 1.0

0	0	0	0.800	0.0	1.0	000.	0.0	0.2
0	0	0	1.000	0.0	1.0	000.	0.0	0.2
0	0	0	1.200	0.0	1.0	000.	0.0	0.2
0	0	0	1.500	0.0	1.0	000.	0.0	0.2
0	0	0	2.000	0.0	1.0	000.	0.0	0.2
0	0	0	3.000	0.0	1.0	000.	0.0	0.2
0	1	0	4.000	0.0	1.0	000.	0.0	0.2
0	1	0	5.000	0.0	1.0	000.	0.0	0.2
0	1	0	6.000	0.0	1.0	000.	0.0	0.2
0	1	0	7.000	0.0	1.0	000.	0.0	0.2
0	1	0	8.000	0.0	1.0	000.	0.0	0.2
0	1	0	10.00	0.0	1.0	000.	0.0	0.2
0	1	0	11.00	0.0	1.0	000.	0.0	0.2
0	1	0	12.00	0.0	1.0	000.	0.0	0.2
0	1	0	13.00	0.0	1.0	000.	0.0	0.2
0	1	0	14.00	0.0	1.0	000.	0.0	0.2
0	1	0	15.00	0.0	1.0	000.	0.0	0.2
0	1	0	16.00	0.0	1.0	000.	0.0	0.2
0	1	0	18.00	0.0	1.0	000.	0.0	0.2
0	1	0	20.00	0.0	1.0	000.	0.0	0.2

***** INPUT ON UNIT 63 *****

```

1242      1      1
0.1      0.01
N,G
  12      0      0      0 102      0      0
243.0      0.0      94.0      0.0      0.0      5.0342
0000 35 +1 2 0058 45 +1 2 0124 55 +1 2 0204 65 +1 2 0288 25 +1 2
0333 35 +1 2 0384 05 +1 2 0392 45 +1 2 0393 15 +1 2 0403 45 -1 2
0447 25 +1 2 0450 35 +1 2
0.46 3.827 -0.511 0.401 27.623 94.66 0.710 2
N,F
5.30      5.10      0.80      0.52
  12

```

0000	35	+1	2	0029	45	+1	2	0062	55	+1	2	0102	65	+1	2	0144	25	+1	2
0166	35	+1	2	0192	05	+1	2	0196	45	+1	2	0194	15	+1	2	0202	45	-1	2
0224	25	+1	2	0225	35	+1	2												
0.226	4.396	-1.068	0.391	32.457	111.2	0.710	2												
12																			
0000	35	+1	2	0029	45	+1	2	0062	55	+1	2	0102	65	+1	2	0144	25	+1	2
0166	35	+1	2	0192	05	+1	2	0196	45	+1	2	0194	15	+1	2	0202	45	-1	2
0224	25	+1	2	0225	35	+1	2												
0.226	4.396	-1.068	0.391	32.457	111.2	0.710	2												
1242	2	1																	

N,NG

20	0	1	0	91															
242.0	0.0		94.0	0.0	0.0	0.0													
0000	00	+1	2	0044	20	+1	2	0147	40	+1	2	0306	60	+1	2	0518	80	+1	2
0779	100	+1	2	0780	10	-1	2	0833	30	-1	2	0865	30	-1	2	0927	50	-1	2
0956	00	+1	2	0986	20	-1	2	0995	20	+1	2	1019	30	-1	2	1040	40	+1	2
1064	40	-1	2	1087	120	+1	2	1102	20	+1	2	1122	50	-1	2	1152	20	-1	2
1.16	4.035	-0.015	0.390	27.797	94.99	1.100	2												

N,2N

10	0	1	1	16	1														
241.0	1.0		94.0	0.0	0.5	-6.3097													
0000	25	+1	2	0041	35	+1	2	0063	45	+1	2	0067	55	+1	2	0094	45	+1	2
0161	05	+1	2	0170	15	+1	2	0174	35	+1	2	0229	45	+1	2	0235	25	+1	2
47.626	-0.344	1.203	0.628	5.913	-0.255	1.306	0.57	1	40										
-0.566	0.210																		
0.24	3.512	-0.676	0.395	27.66	94.26	0.490	2												

N,NF

5.4	5.1	1.04	0.6																
10																			

0000	00	+1	2	0022	20	+1	2	0074	40	+1	2	0153	60	+1	2	0259	80	+1	2
0389	100	+1	2	0390	10	-1	2	0416	30	-1	2	0433	30	-1	2	0463	50	-1	2
0.480	4.847	-0.643	0.418	29.187	99.74	1.100	2												
10																			
0000	00	+1	2	0022	20	+1	2	0074	40	+1	2	0153	60	+1	2	0259	80	+1	2
0389	100	+1	2	0390	10	-1	2	0416	30	-1	2	0433	30	-1	2	0463	50	-1	2
0.480	4.847	-0.643	0.418	29.187	99.74	1.100	2												
1	1	1																	
1242	2	1																	

N2NG

10	0	0	0	0															
241.0	0.0		94.0		0.0		0.0		-6.3097										
0000	25	+1	2	0041	35	+1	2	0063	45	+1	2	0067	55	+1	2	0094	45	+1	2
0161	05	+1	2	0170	15	+1	2	0174	35	+1	2	0229	45	+1	2	0235	25	+1	2
0.24	3.512	-0.676	0.395	27.66	94.26	0.490	2												

N,3N

10	0	0	1	17	1														
240.0	1.0		94.0		0.0		0.5		-11.5512										
0000	00	+1	2	0043	20	+1	2	0142	40	+1	2	0294	60	+1	2	0498	80	+1	2
0597	10	-1	2	0649	30	-1	2	0742	50	-1	2	0861	00	+1	2	0900	20	+1	2
47.626	-0.344	1.203	0.628	5.913	-0.255	1.306	0.57					1	40						
-0.566	0.210																		
1.0	3.654	0.020	0.382	27.083	92.04	0.970	2												

N2NF

5.5	5.1		0.8		0.52														
10																			
0000	25	+1	2	0021	35	+1	2	0032	45	+1	2	0034	55	+1	2	0047	45	+1	2
0081	05	+1	2	0085	15	+1	2	0087	35	+1	2	0115	45	+1	2	0117	25	+1	2
0.12	4.581	-1.487	0.432	29.043	98.98	0.490	2												
10																			
0000	25	+1	2	0021	35	+1	2	0032	45	+1	2	0034	55	+1	2	0047	45	+1	2
0081	05	+1	2	0085	15	+1	2	0087	35	+1	2	0115	45	+1	2	0117	25	+1	2
0.12	4.581	-1.487	0.432	29.043	98.98	0.490	2												

1

INTERNAL DISTRIBUTION

- | | | | |
|------|----------------------|--------|---------------------------------|
| 1. | L. S. Abbott | 19. | F. G. Perey |
| 2. | R. G. Alsmilier, Jr. | 20. | R. W. Roussin |
| 3. | D. G. Cacuci | 21. | R. T. Santoro |
| 4. | J. K. Dickens | 22. | L. W. Weston |
| 5-9. | C. Y. Fu | 23. | A. Zucker |
| 10. | T. A. Gabriel | 24. | P. W. Dickson, Jr. (consultant) |
| 11. | R. Gwin | 25. | G. H. Golub (consultant) |
| 12. | D. T. Ingersoll | 26. | R. M. Haralick (consultant) |
| 13. | D. M. Hetrick | 27. | D. Steiner (consultant) |
| 14. | C. H. Johnson | 28. | Document Reference Section |
| 15. | D. C. Larson | 29. | K-25 Plant Library |
| 16. | F. C. Maienschein | 30-31. | Laboratory Records |
| 17. | B. F. Maskewitz | 32. | ORNL Patent Section |
| 18. | R. W. Peelle | 33. | Laboratory Records-RC |

EXTERNAL DISTRIBUTION

34. E. D. Arthur, T-2, MS243, Los Alamos National Laboratory, P. O. Box 1663, Los Alamos, NM 87545
35. S. E. Berk, G234, Division of Development and Technology, Office of Fusion Energy, U.S. Department of Energy, Washington, DC 20545
36. M. R. Bhat, Building 197D, National Nuclear Data Center, Brookhaven National Laboratory, Upton, NY 11973
37. Chief, Mathematics and Geoscience Branch, U.S. Department of Energy, Washington, DC 20545
38. Herbert Goldstein, 211 Mudd Columbia University, 520 West 120th St., New York, NY 10027
39. D. G. Gardner, P. O. Box 808, Lawrence Livermore National Laboratory, Livermore, CA 94550
40. Robert MacFarlane, T-2, MS243, Los Alamos National Laboratory, P. O. Box 1663, Los Alamos, NM 87545
41. D. G. Madland, Los Alamos National Laboratory, P. O. Box 1663, Los Alamos, NM 87545
42. Roger White, Los Alamos National Laboratory, P. O. Box 1663, Los Alamos, NM 87545
43. F. M. Mann, W/A-4, Westinghouse Hanford, P. O. Box 1970, Washington, DC 99352
44. Robert Schenter, Westinghouse Hanford, P. O. Box 1970, Washington, DC 99352
45. D. L. Smith, Building 314, Applied Physics Division, Argonne National Laboratory, 9700 South Cass Ave., Argonne, IL 60439
46. Stanley Whetstone, Division of Nuclear Sciences, Office of Basic Energy Sciences, U.S. Department of Energy, Washington, DC 20545
47. Phillip Young, T-2, MS-243, Los Alamos National Laboratory, P. O. Box 1663, Los Alamos, NM 87545
48. J. G. Campbell, Defense Nuclear Agency, Washington, DC 20305
49. Harm Gruppelaar, Netherland Energy Research Foundation ECN, P. O. Box 1, NL-1755 ZG, Petten NH, The Netherlands

50. **Kichinosuke Harada, Director, Department of Physics, Japan Atomic Energy Research Institute, Tokai Research Establishment, Tokai-mura, Naga-gun, Isaraki-ken, Japan**
- 51-55. **K. Shibata, Nuclear Data Center, Japan Atomic Energy Research Institute, Tokai-mura, Ibaraki-ken 319-11, Japan**
56. **Office of Assistant Manager for Energy Research and Development, U.S. Department of Energy, Oak Ridge Operations, Oak Ridge, TN 37831**
- 57-83. **Technical Information Center, Oak Ridge, TN 37831**